11th World Congress on Computational Mechanics (WCCM XI)
5th European Conference on Computational Mechanics (ECCM V)
6th European Conference on Computational Fluid Dynamics (ECFD VI)
E. Oñate, J. Oliver and A. Huerta (Eds)

FULL WAVEFORM INVERSION IN MIGRATION BASED TRAVEL TIME FORMULATION

Guy Chavent[1], Kirill Gadylshin[2,3,*] and Vladimir Tcheverda[3]

[1] Inria-Rocquencourt, Domaine de Voluceau,
BP 105, 78153 Le Chesnay Cedex, France
[2] Novosibirsk State University, Mechanics and Mathematics Department
Pirogova 2, 630090 Novosibirsk, Russia
[3] Institute of Petroleum Geology and Geophysics, SB RAS
Prosp. Akademika Koptyuga 3, 630090 Novosibirsk, Russia
*Email: GadylshinKG@ipgg.sbras.ru

Key words: seismic imaging, wave propagation, inverse problems, full waveform inversion

Abstract. The common knowledge now is that standard least squares Full Waveform Inversion is unable to reconstruct macrovelocity for reasonable frequency band of input data but claims unpractically low time frequencies. There are a range of different approaches to overcome this weakness and among them Migration Based Travel Time reformulation of the cost function. Here we compare standard least squares Full Waveform Inversion with its Migration Based Travel Time reformulation. Our computations demonstrate the reliable reconstruction of the smooth velocity component by full waveform inversion in migration based travel-time formulation.

1 Introduction

Constructing a smooth velocity model (propagator, macro velocity constituent) in the depth domain, which is responsible for correct travel-times of wave propagation is a key element of the up-to-date seismic data processing in areas with complex local geology. Theoretically it could be obtained, along with the subsurface structure, by the Full Waveform Inversion (FWI) technique matching the observed and the synthetic seismograms (Tarantola, 1984). The L_2 norm is usually used for this matching, though other criteria are also considered. To minimize the misfit function and to find the elastic parameters of the subsurface, iterative gradient-based algorithms are usually applied. Such approach to solving seismic inverse problem proposed originally by Tarantola (1984) has been developed and studied in a great number of publications (see Virieux and Operto, 2009, and the references therein).

However, the straightforward application of FWI reconstructs reliably only the reflectivity component of the subsurface but fails to provide a smooth velocity (propagator) component of a model. In order to overcome this trouble G.Chavent with colleagues introduced Full Waveform Inversion in Migration Based Travel-Time formulation (2001). The main idea of this approach is to decompose model space into two orthogonal subspaces - smooth propagator and rough reflector with subsequent reformulation of the cost function.

2 Methods

2.1 Statement

Full Waveform Inversion formally is application of non-linear least squares for seismic inverse problem treated as a nonlinear operator equation

$$\mathcal{F}[m] = d. \tag{1}$$

Here the known right-hand side d is multi-source multi-receivers seismic data, $\mathcal{F}$ is a non-linear operator (forward map) which transforms the current model m to synthetic data. For the sake of simplicity we deal with the Helmholtz equation:

$$\Delta u + \frac{\omega^2}{c(x)^2} u = f(\omega)\delta(x - x_s)$$

with data d being its solution computed at receivers positions.

Instead of regular non-linear least squares formulation of Full Waveform Inversion, when unknown function $c(x)$ is searched as

$$c_* = \underset{c}{argmin} \, \|d - \mathcal{F}(c)\|^2, \tag{2}$$

MBTT introduces the following decomposition of the model space:

$$m = p + r = p + \Pi_r \mathcal{M}(p) < s > . \tag{3}$$

Here $p \in P$ describes smooth macrovelocity, which does not perturb significantly direction of waves propagation, but governs their travel times. In contrast the **depth reflector** r describes rough perturbations of the model, which send seismic energy back to the surface, but do not change travel-times. The key moment here is interrelation $r = \Pi_r \mathcal{M}(p) < s >$ where s is unknown **time reflectivity**, $\mathcal{M}(p)$ - a true amplitude prestack migration operator with linear reweighing W and Π_r is the orthogonal projector onto the space of reflectors (orthogonal to the space of propagators). In more details this operator is written down as

$$\mathcal{M}(p) < s >= W \circ Re \left\{ \left(\frac{\delta \mathcal{F}}{\delta m}(p) \right)^* < s > \right\}, \tag{4}$$

where * denotes adjoint operator in application to Frechet derivative of nonlinear forward map $\mathcal{F}$.

In this notations MBTT formulation of FWI with respect to propagator p and time reflectivity s is as follows:

$$(p^*, s^*) = \underset{p,s}{argmin} \, \|d - \mathcal{F}(p + \Pi_r \mathcal{M}(p) < s >)\| \tag{5}$$

2.2 Non-linear inversion with respect to propagator unknown

Consider the modified objective function $\widetilde{E}(p; s)$:

$$\widetilde{E}(p; s) = \|d - \mathcal{F}(p + \Pi_r \mathcal{M}(p) < s >)\| \tag{6}$$

One can show that the gradient $\nabla_p \widetilde{E}(p; s)$ is as follows:

$$\nabla_p = Re \left\{ \left(\frac{\delta F}{\delta m}(m) \right)^* \left[F(m) - d^{obs} \right] + \right. \tag{7}$$
$$\left. \frac{\delta^2 F}{\delta m^2}(p) \left[\cdot \, , W^* \circ \left(\frac{\delta F}{\delta m}(m) \right)^* \left[F(m) - d^{obs} \right] \right]^* [s] \right\}$$

where $m = p + \Pi_r \mathcal{M}(p) < s >$.

Application of the conjugate gradient (CG) method for minimizing of $\widetilde{E}(p; s)$ with respect to a propagator unknown gives the following iteration process:

$$p_{k+1} = p_k + \mu_k S_k \tag{8}$$

where p_k - propagator on each step, $\mu_k \in \mathbb{R}$ is a step length of the propagator update and the S_k is a direction of the propagator update of the following form:

$$S_k = -\nabla_k - \frac{\langle \nabla_k, \nabla_k - \nabla_{k-1} \rangle_M}{\langle \nabla_{k-1}, \nabla_{k-1} \rangle_M} S_{k-1}, \tag{9}$$

where $\nabla_k = \nabla \widetilde{E}(p_k; s)$. Using second order approximation to the objective function the step length of propagator update can be found as:

$$\mu_k = -\frac{\langle \nabla_k, S_k \rangle_M}{\langle L_k < S_k >, L_k < S_k > \rangle_D}, \tag{10}$$

where L_k is a Freche't derivative with respect to p of the modified forward map calculated at the point $(p_k; s)$:

$$L_k = \frac{\delta}{\delta p} \mathcal{F}(p_k + \Pi_r \mathcal{M}(p_k) < s >) \tag{11}$$

2.3 Non-linear inversion with respect to time-reflectivity unknown

In order to implement the full cycle of MBTT inversion one also need minimize the modified objective function $\widetilde{E}(p;s)$ with respect to the time-reflectivity unknown. The gradient $\nabla_s \widetilde{E}(p;s)$ can be found as follows:

$$\nabla_s = -\frac{\delta F}{\delta m}(p)\left[W^* \circ \frac{\delta F}{\delta m}^*(m)\left\langle d^{obs} - F(m)\right\rangle\right]. \tag{12}$$

Application of the steepest descent method for minimizing of $\widetilde{E}(p;s)$ with respect to a time-reflectivity unknown gives the following iteration process:

$$s^{k+1} = s^k - \mu_k \nabla_{s^k}, \tag{13}$$

where s_k - time-reflectivity on each step, $\mu_k \in \mathbb{R}$ is a step length of the time-reflectivity update. The choice of the step length μ_k in (13) is crucial for the convergence of the steepest gradient optimization method. For three test step lengths 0 , α_1 and α_2 three values of objective function are calculated

$$\begin{aligned} E_0 &= \widetilde{E}(p;s^k), \\ E_1 &= \widetilde{E}(p;s^k - \alpha_1 \nabla_{s^k}), \\ E_2 &= \widetilde{E}(p;s^k - \alpha_2 \nabla_{s^k}). \end{aligned} \tag{14}$$

Assume that locally around s^k the true misfit function can be approximated by fitting a parabola through the three points $\{0, \alpha_1, \alpha_2\}$:

$$\widetilde{E}(p;s^k - \alpha \nabla_{s^k}) = a\alpha^2 + b\alpha + c, \tag{15}$$

then we have the following SLAE for (a,b,c):

$$\begin{aligned} c &= E_0, \\ a\alpha_1^2 + b\alpha_1 + c &= E_1, \\ a\alpha_2^2 + b\alpha_2 + c &= E_2. \end{aligned} \tag{16}$$

Finally the optimal step on $k-th$ iteration:

$$\mu_k = -\frac{b}{2a}. \tag{17}$$

3 Numerical experiments

Consider the layered velocity model m_{true} presented on Fig. 1. The initial guess m_0 is constant up to the depth 100 m and a linear function (with respect to the depth) starting from 100 m up to the depth 1500 m:

$$m_0(x,z) = \begin{cases} 3000 \text{ m/s}, & \text{if } z \le 100 \\ \frac{3}{14}(z-100) + 3000 \text{ m/s}, & \text{if } z > 100 \end{cases} \tag{18}$$

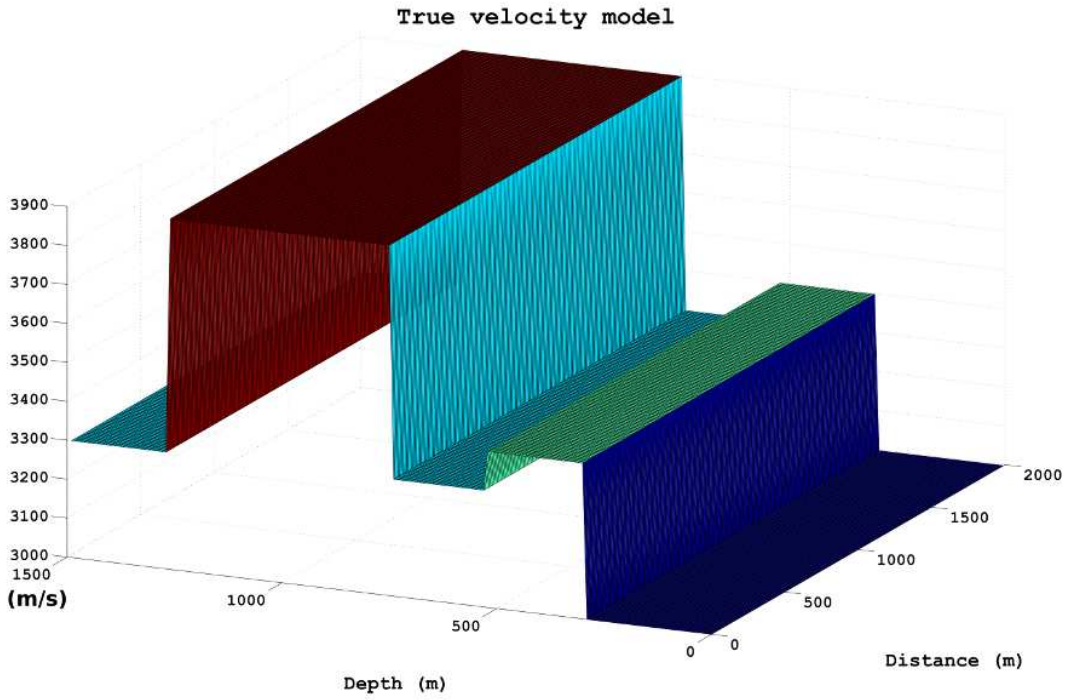

Figure 1: True velocity distribution m_{true}.

The acquisition system contains 25 volumetric point-sources and 99 receivers placed evenly on the top of the model.The frequency band of input data consists of 207 frequencies placed evenly in the segment $[7, 40]$ Hz and the source impulse - Ricker wavelet with dominant frequency 15 Hz.

Let us start from the classical L_2 inversion providing we use m_0 as a start model for non-linear iterations via CG method. The inversion results (Fig. 2) demonstrate the main weaknesses of the standard inversion approach: local minima of the objective functional and slow convergence. As one can see the macrovelocity component of the solution is not recovered. Instead of smooth component, mainly the reflectors are presented in the solution, but if for the top layers the interfaces appear on the correct places then for the deeper layers the interfaces are recovered on the wrong positions (the last interface is recovered with error 200 m).

We propose the minimization scheme presented on Fig. 3 as a minimization algorithm for inversion in MBTT formulation. On first stage we update the time-reflectivity, then on the second stage - propagator. Then we repeat the loop again. The results of MBTT inversion are presented on Fig. 4

Since recovered full model is very close to the true solution we suggest to run stardard L_2 inversion using recovered on MBTT stage model as a start model. Results of such experiment are presented on Fig. 5. On Fig. 6 we present time-domain data residuals

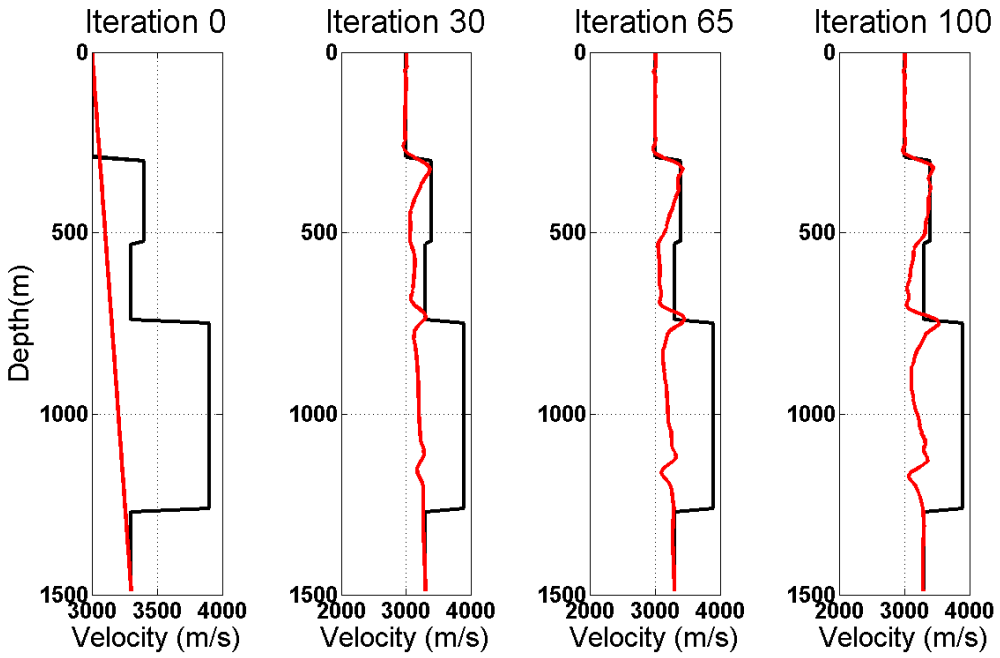

Figure 2: Classical inversion results. Red plot - recovered model on current iteration, black plot - true model.

for models obtained after CLS inversion but for different initial guesses: in the first case we use m_0 and in the second case - model recovered after MBTT inversion. One may recognize almost perfect reconstruction of full model, when we apply standard inversion technique after MBTT inversion and as a result we have the better data explanation (time-domain data residuals are smaller when we use MBTT before classical inversion).

The last experiment - sequential classical single frequency inversion. Starting single frequency inversion from 5Hz we use the model recovered on 5Hz as a start model for 6Hz inversion and so on up to the 10Hz. The following set of frequencies were used during inversion: 5Hz, 6Hz, 7Hz and 10Hz. The results of sequential inversion are presented on Fig. 7.

4 Conclusions

We introduced MBTT formulation in frequency domain. In case of MBTT formulation the low-frequency components of the solution are presented in recovered models, as opposed to the standard L_2 approach. Presented numerical examples prove the feasibility of MBTT technique for recovering the smooth component of the solution in case of absence low frequencies in the observed data (lower frequency 7Hz).

The computations were performed on the HERMIT supercomputer of the High Performance Computing Center Stuttgart under the PRACE consortium grant 2012071274. The research was done under financial support of the Russian Foundation for Basic Re-

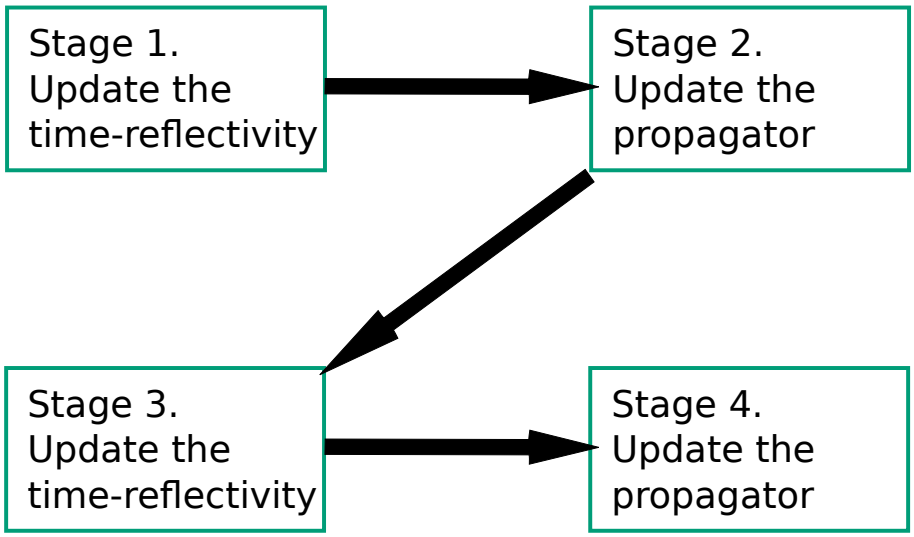

Figure 3: MBTT minimization algorithm.

search grants no. 13-05-12051, 14-05-31257, 14-05-00109, 14-05-00049, 14-05-93090, grant MK-2909.2014.5 of the President of the Russian Federation, and integration projects of SB RAS 127 and 130.

REFERENCES

[1] F. Clement, G. Chavent, and S. Gomez. Migration-based traveltime waveform inversion of 2-d simple structures: A synthetic example. *Geophysics*, 66:845–860, 2001.

[2] A. Tarantola. Inversion of seismic reflection data in the acoustic approximation. *Geophysics*, 49(8):12591266, 1984.

[3] J. Virieux and S. Operto. An overview of full-waveform inversion in exploration geophysics. *Geophysics*, 74(6):WCC1 – WCC26, 2009.

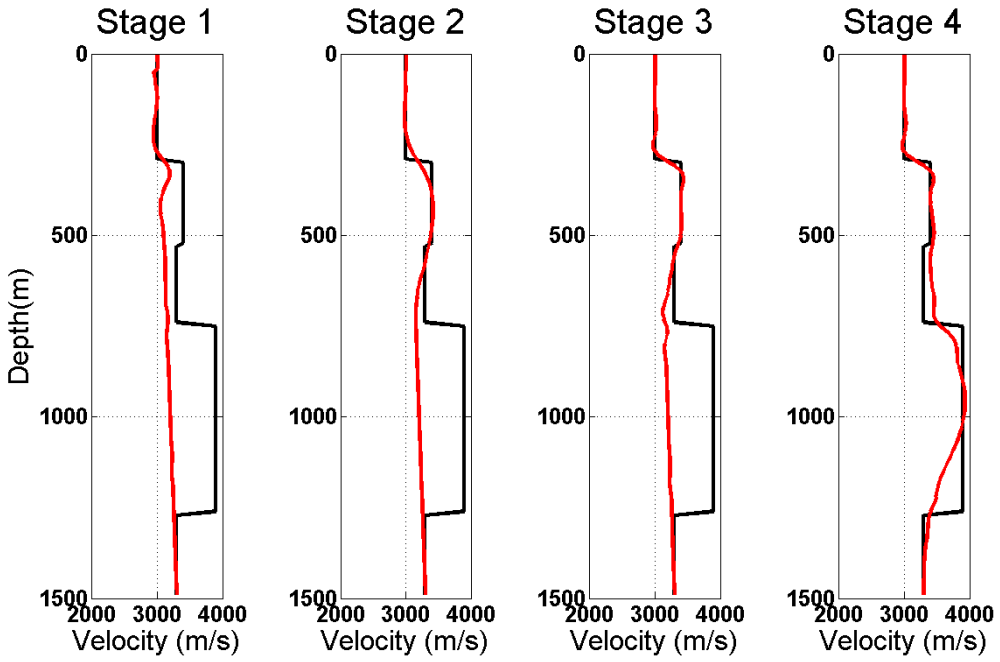

Figure 4: MBTT inversion results. Red plot - recovered model on current stage, black plot - true model.

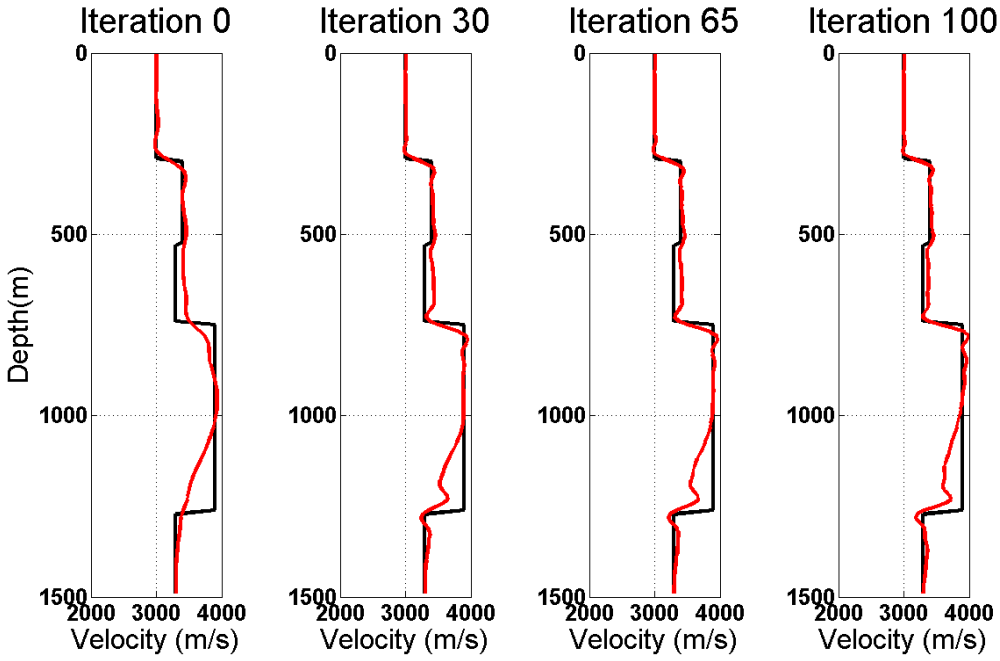

Figure 5: Classical inversion using model obtained after MBTT inversion as initial guess

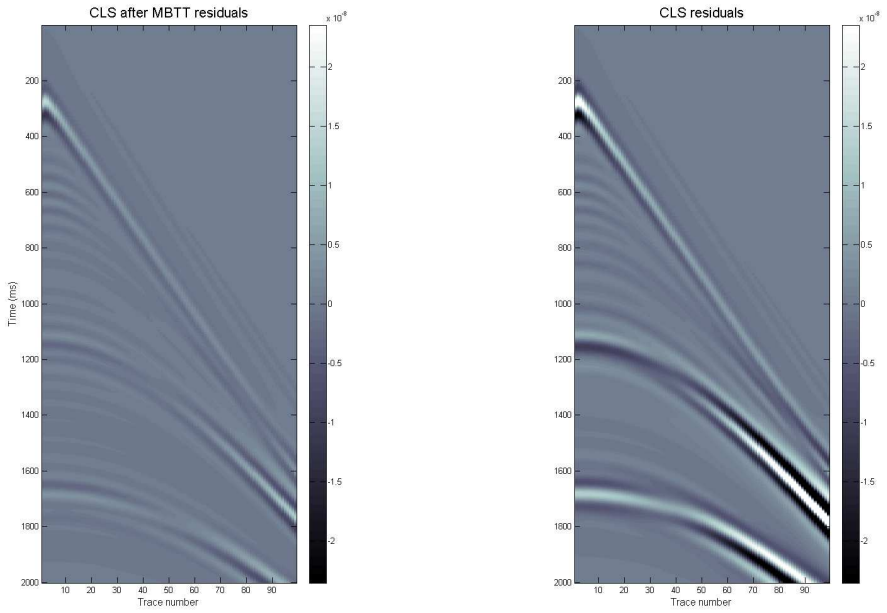

Figure 6: Time-domain data residuals. Left - classical inversion after MBTT, right - classical inversion.

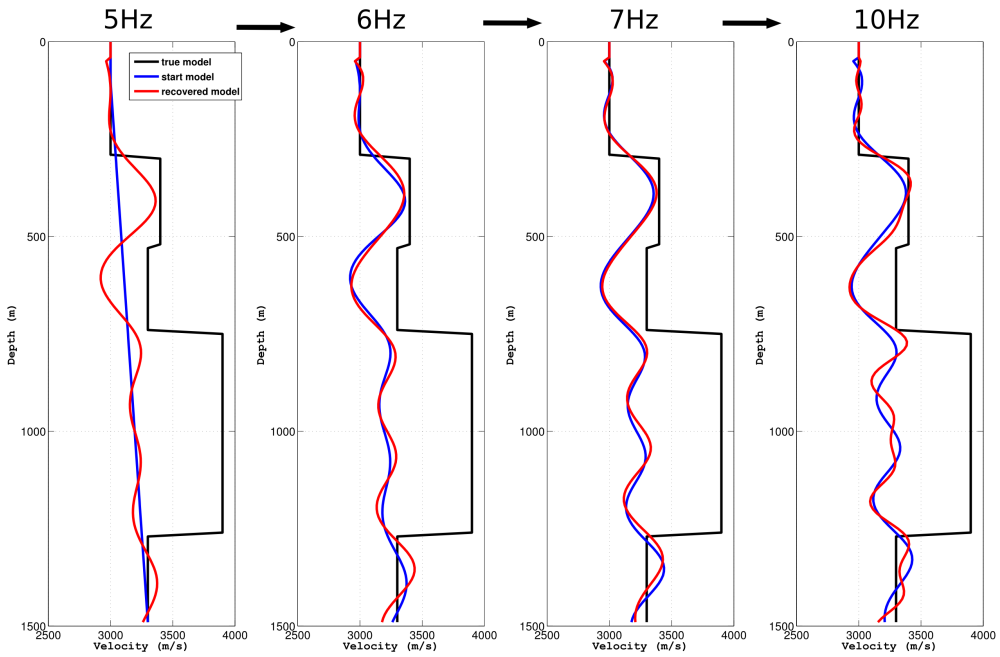

Figure 7: Sequential classical inversion starting from 5Hz.